

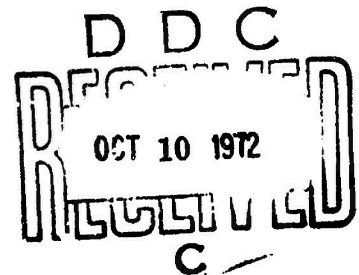
AD 749362

EFFECT OF GAS PROPERTIES ON THE PERMEABILITY
OF FINE-PORED CARBONS

by Bahram Keramati

Technical Memorandum
File No. TM 72-120
July 12, 1972
Contract No. N00017-70-C-1407

Copy No. 8



The Pennsylvania State University
Institute for Science and Engineering
ORDNANCE RESEARCH LABORATORY
University Park, Pennsylvania

Reproduced by
NATIONAL TECHNICAL
INFORMATION SERVICE
U.S. Department of Commerce
Springfield, VA 22151

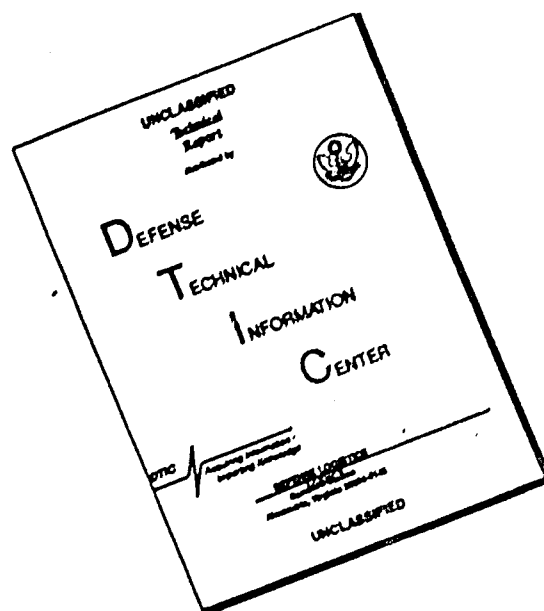
NAVY DEPARTMENT

NAVAL ORDNANCE SYSTEMS COMMAND

DISSEMINATION
DOCUMENTS
UNCLASSIFIED

268

DISCLAIMER NOTICE



THIS DOCUMENT IS BEST QUALITY AVAILABLE. THE COPY FURNISHED TO DTIC CONTAINED A SIGNIFICANT NUMBER OF PAGES WHICH DO NOT REPRODUCE LEGIBLY.

UNCLASSIFIED

- 2 -

July 12, 1972
MTP:dlt

ABSTRACT

The permeability of two fine-pored carbons were experimentally determined as a function of the mean pressure, temperature, temperature gradient and gas properties. The gases used in the investigation were helium, nitrogen, argon and sulfur hexafluoride. It was found that permeability is not only a function of the mean pressure, but is also dependent on the inlet pressure. A mean temperature increase, however, was found to decrease the permeability. The application of two previously proposed models did not lead to an accurate prediction of the effect of gas properties on the flow. A new correlation which predicts most of the experimentally determined permeabilities within 7% was presented. The experimental data of other investigators were also shown to be predictable by this correlation.

I-8

UNCLASSIFIED

ACKNOWLEDGMENTS

The guidance and direction of Dr. Carl H. Wolgemuth were essential during the course of this investigation and the preparation of the thesis. To him the author extends his gratitude.

Appreciation is also due the Ordnance Research Laboratory of The Pennsylvania State University under contract with Naval Ordnance Systems Command, for the financial support of this research effort.

DOCUMENT CONTROL DATA - R & D		
(Security classification of title, abstract and indexing annotation when overall report is classified)		
1. ORIGINATING ACTIVITY (Corporate author)		2a. REPORT SECURITY CLASSIFICATION
Ordnance Research Laboratory University Park, Pennsylvania		Unclassified
		2b. GROUP
3. REPORT TITLE		
Effect of Gas Properties on the Permeability of Fine-Pored Carbons		
4. DESCRIPTIVE NOTES (Type of report and inclusive dates)		
M.S. Thesis, Mechanical Engineering, September 1972		
5. AUTHOR(S) (First name, middle initial, last name)		
Bahram Keramati		
6. REPORT DATE	7a. TOTAL NO. OF PAGES	7b. NO. OF REFS
July 12, 1972	68	13
8a. CONTRACT OR GRANT NO.	9a. ORIGINATOR'S REPORT NUMBER(S)	
N00017-70-C-1407	TM 72-120	
b. PROJECT NO.	9b. OTHER REPORT NO(S) (Any other numbers that may be assigned this report)	
c.		
d.		
10. DISTRIBUTION STATEMENT		
Approved for public release. Distribution unlimited. Per NAVORD - June 7, 1972		
11. SUPPLEMENTARY NOTES		12. SPONSORING MILITARY ACTIVITY
		Naval Ordnance Systems Command Department of the Navy
13. ABSTRACT		
<p>The permeability of two fine-pored carbons were experimentally determined as a function of the mean pressure, temperature, temperature gradient and gas properties. The gases used in the investigation were helium, nitrogen, argon and sulfur hexafluoride. It was found that permeability is not only a function of the mean pressure, but is also dependent on the inlet pressure. Temperature gradient itself did not appreciably affect the flow. A mean temperature increase, however, was found to decrease the permeability. The application of two previously proposed models did not lead to an accurate prediction of the effect of gas properties on the flow. A new correlation which predicts most of the experimentally determined permeabilities within 7% was presented. The experimental data of other investigators were also shown to be predictable by this correlation.</p>		

14.	KEY WORDS	LINK A		LINK B		LINK C	
		ROLE	WT	ROLE	WT	ROLE	WT
	ARGON	8					
	FINE-PORED CARBONS	8					
	GAS PROPERTIES	8					
	HELIUM	8					
	INLET PRESSURE	8					
	MEAN PRESSURE	8					
	NITROGEN	8					
	PERMEABILITY	8					
	SULFUR HEXAFLUORIDE	8					
	TEMPERATURE	8					
	TEMPERATURE GRADIENT	8					

I-B

TABLE OF CONTENTS

	<u>Page</u>
ACKNOWLEDGMENTS	11
LIST OF TABLES.	v
LIST OF FIGURES	vi
NOMENCLATURE.	vii
ABSTRACT.	ix
I. INTRODUCTION	1
1.1 Problem Statement	1
1.2 The Porous Carbon	1
1.3 Physical Aspects of Flow.	2
II. REVIEW OF PREVIOUS WORK.	4
2.1 Introduction.	4
2.2 Available Models.	5
2.3 A Critical Review of Available Models	9
2.4 Implications of Previous Investigations	11
III. EXPERIMENTAL APPARATUS AND PROCEDURE	13
3.1 Introduction.	13
3.2 The Apparatus	13
3.3 The Porous Samples.	17
3.4 The Gases	18
3.5 Experimental Procedure.	21
3.6 Measurement Errors.	22
IV. EXPERIMENTAL RESULTS	24
V. DEPENDENCE OF PERMEABILITY ON GAS PROPERTIES	35
5.1 Introduction.	35
5.2 Application of Existing Models.	35
5.3 A New Experimental Correlation.	38
5.4 Proposed Correlation Applied to Other Data.	45
VI. SUMMARY AND CONCLUSION	49
6.1 Summary	49
6.2 Conclusion.	49
6.3 Recommendations for Additional Work	50

TABLE OF CONTENTS (CONTINUED)

	<u>Page</u>
BIBLIOGRAPHY.	52
APPENDIX: EXPERIMENTAL DATA.	53

LIST OF TABLES

<u>Table</u>	<u>Title</u>	<u>Page</u>
1	Properties of the Gases Used in the Investigation . . .	18
2	Significant Gas Parameters in Flow Through FC-01 and FC-25 at Room Temperature and 0.7 atm. Pressure	34
3	Values of B_0 and K_0 For FC-01	36
4	Values of B_0 and K_0 for FC-25	36
5	Values of N Using Somerville's Model for FC-25.	37
6	Significant Gas and Flow Parameters	40
7	Values of A_0 and α for FC-01 and FC-25 Carbons.	45

LIST OF FIGURES

<u>Figure</u>	<u>Caption</u>	<u>Page</u>
1	Schematic Diagram of Experimental Set-Up.	14
2	Test Cell Components.	16
3	Results of the Mercury Porosimetry Test for FC-01 . . .	19
4	Results of the Mercury Porosimetry Test for FC-25 . . .	20
5	Mass Flow Rate of Argon in FC-01 Versus Pressure Drop .	25
6	Permeability Versus Mean Pressure for Flow of Argon in FC-01.	27
7	Mass Flow Rate of Argon in FC-25 Versus Pressure Drop .	28
8	Permeability Versus Mean Pressure for Flow of Argon in FC-25.	29
9	Isothermal Mass Flow Rates Versus Pressure Drop in FC-25.	31
10	Permeability Versus Mean Pressure in FC-01.	32
11	Permeability Versus Mean Pressure in FC-25.	33
12	$\lambda_m K$ Versus Molecular Weight for FC-25	42
13	$\lambda_m K$ Versus Molecular Weight for FC-01	44
14	Permeability Versus Mean Molecular Speed, from Barrer and Strachan's Data [11]	46
15	λ (298°K, 1 atm.)K Versus Molecular Weight, from Barrer and Strachan's Data [11]	48

NOMENCLATURE

<u>Symbol</u>	<u>Description</u>
A	Cross sectional flow area of the porous carbon sample, cm^2
A_0	Porous medium constant, cm^3/min or cm^3/sec
a	Pore radius, cm
B_0	Porous medium constant, cm^2
d	Pore diameter, cm
K	Permeability, cm^2/min or cm^2/sec
K_0	Porous medium constant, cm
k	Porous medium constant, dimensionless
k_0	Porous medium constant, dimensionless
k_1	Porous medium shape factor, dimensionless
k_t	Tortuosity, dimensionless
k'	Porous medium constant, dimensionless
Kn	Knudsen number, dimensionless
L	Porous carbon dimension in the direction of flow, cm
M	Molecular weight, gm/mole
\dot{m}	Mass flow rate, gm/min
N	Number of stacked planes in Somerville's model, dimensionless
p	Pressure, in. Hg or psia or atm.
Q	Volume flow rate, cm^3/min
R	Universal gas constant, $= 8.3147 \times 10^7$, ergs/ $^\circ\text{K}$ -mole
S	Total internal pore area, cm^2
T	Temperature, $^\circ\text{K}$
\bar{v}	Mean molecular thermal speed, cm/sec

NOMENCLATURE (Continued)

<u>Symbol</u>	<u>Description</u>
x	Distance from the inlet through the porous sample, cm
Z	Compressibility factor, dimensionless
<u>Greek Letters</u>	
α	Porous medium constant, dimensionless
δ	Coefficient allowing for specular reflection of gas molecules, dimensionless
ϵ	Porosity, dimensionless
η	Viscosity, gm/cm-sec
λ	Mean free path, cm
ρ	Density, gm/cm ³
ϕ	Effective pore area distribution, dimensionless
ϕ_o	Cumulative pore area distribution on surface, dimensionless
ϕ_m	Specific pore area, dimensionless
<u>Subscripts</u>	
m	Refers to a mean value
in	Refers to the inlet

ABSTRACT

The permeability of two fine-pored carbons was experimentally determined as a function of the mean pressure, temperature, temperature gradient and gas properties. The gases used in the investigation were helium, nitrogen, argon and sulfur hexafluoride. It was found that permeability is not only a function of the mean pressure, but is also dependent on the inlet pressure. Temperature gradient itself did not appreciably affect the flow. A mean temperature increase, however, was found to decrease the permeability. The application of two previously proposed models did not lead to an accurate prediction of the effect of gas properties on the flow. A new correlation technique which predicts most of the experimentally determined permeabilities within 7% was presented. The experimental data of other investigators was also shown to be predictable by this correlation.

CHAPTER I

INTRODUCTION

1.1 Problem Statement

Fine-pored carbons possess many unique properties suitable for a variety of industrial applications. For example, their mechanical strength, electrical conductivity and permeability to the flow of gases form the basis for their use as fuel cell cathodes. The power density of a fuel cell is dependent on the flow rate of the oxidant gas through the cathode matrix. Due to the heat generated in the fuel cell, a temperature gradient usually exists in the porous carbon cathode. A knowledge of the permeability of the carbon as a function of pressure, temperature gradient and gas properties, therefore, is of primary importance in this application.

The purpose of this research effort is the experimental determination of the effect of gas properties on the permeability of fine-pored, consolidated carbons under isothermal and non-isothermal conditions. The effort will be restricted to steady flow situations.

1.2 The Porous Carbon

Due to the complexity of the structure of consolidated, porous carbons, an exact characterization of the medium is practically impossible. Some measurable carbon characteristics, however, have been found to have a direct influence on the flow

phenomena. These include porosity, total internal surface area, and pore size distribution. Unconnected pores (voids) and dead-ended pores are also of importance.

Mercury porosimetry, the scanning electron microscope, and absorption tests have been used to characterize porous media. In the mercury porosimetry technique, mercury is forced through an evacuated sample of the porous carbon and the volume of the penetrated mercury is measured as a function of its pressure. The results of this measurement, together with certain assumptions regarding the shape of the pores and the contact angle of mercury in the pores, lead to a knowledge of the sample's pore size distribution. A complete description of the mercury porosimetry technique which is the most widely-used method is given by Orr [1]. Inherent errors involved in relating the results of this technique to the structure of the sample are examined by Bickerman [2]. Somerville [3] has investigated the use of the scanning electron microscope in characterizing porous carbons, and compares pore size distribution results with those given by mercury porosimetry.

1.3 Physical Aspects of Flow

The character of the flow of gas in a given pore depends on the Knudsen number, Kn , defined as

$$Kn = \frac{d}{\lambda} , \quad (1.1)$$

where d is the pore diameter and λ is the mean free path of the gas in that pore. For large values of Kn (larger than 10), molecule-molecule collisions are much more frequent than molecule-wall

collisions, and the gas may be treated as a continuum. In this flow regime, the important gas parameter is the viscosity. At very low pressures, where molecule-molecule collisions may be neglected compared with molecule-wall collisions, the Knudsen number is small (less than 0.01), and viscosity loses its significance. In this regime, known as the free molecular regime, the average molecular velocity, \bar{v} , which is inversely proportional to the square root of the molecular weight, becomes important to the flow phenomena.

Between these two extremes, when Kn is of the order of unity, transition phenomena occur where both \bar{v} and η are important. Near continuum transition flows are also known as slip flows where the gas may be treated as a continuum with the allowance of a finite velocity at the boundaries.

In a porous medium, all these flow regimes may be realized in parallel. As the gas pressure decreases through the medium in the direction of the flow, rarefied gas effects become more and more pronounced. Any realistic flow model should take these variations into account.

Physical adsorption, which is significant at low temperatures and high pressures, may also occur in a porous medium. This phenomenon may affect the flow of the gas by reducing the effective areas available for the flow and altering the nature of molecule-wall interactions

CHAPTER II

REVIEW OF PREVIOUS WORK

2.1 Introduction

The problem of modelling gaseous flow phenomena in fine-pored carbons is twofold. On the one hand, equations for the flow of the gas applicable over the entire Knudsen number range must be written and, on the other hand, the proper boundary conditions for these equations must be specified. The former deals with the gas with specific reference to the variation of its transport properties with the Knudsen number, whereas the latter involves the complex geometry and surface characteristics of the porous material.

In the limits of very large and very small Knudsen numbers, the behavior of the gas is fairly well understood. For large values of Kn , the Navier-Stokes equations are applicable, while for small Knudsen numbers, the Maxwellian distribution function leads to an adequate description of the gas.

For moderate values of Kn , considerable difficulties are involved in the formulation of solvable equations for the flow of gases. Although this is a matter of current research, several solutions for simple boundary conditions, such as the one given by Cha and McCoy [4], are available.

Due to the complex structure of consolidated porous carbons, an exact specification of boundary conditions is impractical, if not impossible. Even if the exact structure of the porous

material were known, it would be exceedingly difficult to incorporate this knowledge with the flow equations systematically. Consequently, the classical approach of using appropriate flow equations with the necessary boundary conditions to solve for gaseous flow through porous media has not been attempted.

2.2 Available Models

To date, all attempts have been restricted to the development of simplified models for the carbon, and most of these involve the equations for gaseous flow in tubes. Various models have been proposed for the porous medium which may be classified as follows: models based on capillary tube bundles, first proposed by Adzumi [5]; statistical descriptions of the porous material as proposed by Childs and Collis-George [6]; and the "dusty gas" model given by Evans, Watson and Mason [7]. For the case of thermal diffusion, where a mass flux is obtained by imposing a temperature gradient on a fine-pored sample, the work of Lammers [8] which is based on the methods of irreversible thermodynamics, is available.

A very useful quantity in the study of gross flow characteristics through porous media is the permeability, K , defined as follows:

$$K = \frac{Q_m p_m}{A \left(\frac{\Delta p}{L} \right)}, \quad (2.1)$$

where p_m is the arithmetic mean of the inlet and outlet pressures, Q_m is the volume flow rate at p_m , A is the sample area, Δp is the pressure drop and L is the sample thickness. At a given

temperature, permeability may be thought of as the flow per unit sample area, per unit pressure gradient. In general, for a given gas, permeability would be a function of inlet temperature, temperature gradient, inlet pressure and mean pressure. These parameters, together with the size of a pore and the viscosity and molecular weight of the gas, uniquely determine the flow regime in that pore.

With particular reference to fine-pored carbons, where large and small Knudsen numbers may be encountered simultaneously, Carman and Arnell [9] developed a model for the permeability based on the capillary tube concept. Here, permeability is related to the mean pressure, temperature, viscosity and the mean thermal speed of the gas molecules, \bar{v} , as follows:

$$K = \frac{B_o}{\eta} p_m + \frac{4}{3} K_o \bar{v} \quad , \quad (2.2)$$

where

$$\bar{v} = \left(\frac{8RT}{\pi M} \right)^{1/2} \quad , \quad (2.3)$$

$$B_o = \frac{\epsilon^3}{kS^2} \quad , \quad \text{cm}^2 \quad , \quad (2.4a)$$

$$K_o = \frac{\delta \epsilon^2}{k'S} \quad , \quad \text{cm} \quad (2.4b)$$

and the factors $k' = k_t^2 k_1$ and $k = k_t^2 k_o$. The quantity k_t , known as the tortuosity is defined as the ratio of the actual length of the path a typical molecule travels through the porous sample to the thickness of the sample. δ is a varying coefficient allowing for specular reflection of molecules from the pore walls, k_1 is a shape factor and k_o is the Kozeny constant.

As implied in their definitions, the quantities B_0 and K_0 are dependent on the porous medium alone. The former indicates the contribution of the viscous portion of the flow to the total permeability, and the latter indicates the contribution of the free molecule portion. It is expected that Equation (2.2) will be applicable over the entire Knudsen number range in the case of isothermal flows.

Regarding the models in which a statistical or probabilistic description of the porous medium is attempted, the most recent and the most successful one is that proposed by Somerville [3]. Here, the medium is assumed to be isotropic, i.e., the pore area distribution on any plane within the material is the same. Zero thickness planes having this characteristic pore area distribution, inferred from mercury porosimetry tests, are then conceptually stacked one behind the other in a random fashion until the desired flow resistance of the porous medium is achieved. Thus, an effective pore area distribution representative of the sample is obtained in which the influence of the smaller pores is considerably greater than that of the larger ones as compared with the original pore area distribution on a plane.

To describe the effective pore area distribution mathematically, consider the cumulative pore area distribution on the surface of the porous carbon. This distribution is denoted by $\phi_0(a)$, where a is the radius of a pore. The function $\phi_0(a)$ represents the fraction of the surface area occupied by pores of radius a or larger. If the ratio of the total pore area to the geometric surface area is

denoted by ϕ_m , the ratio $\phi_o(a)/\phi_m$ represents the fraction of pores on the carbon surface having radius a or larger.

The probability that a gas molecule enters the sample through a pore of radius a or larger is given by $\phi_o(a)$. The probability that the same gas molecule travels through N stacked planes, each having a cumulative pore area distribution $\phi_o(a)$, is given by

$$\left[\phi_o(a)/\phi_m \right]^N \quad (2.5)$$

The product of these two probabilities, $\phi(a)$, given by

$$\phi(a) = \phi_o(a) \left[\phi_o(a)/\phi_m \right]^N \quad (2.6)$$

is then the probability that a gas molecule enters the porous carbon through a pore of radius a or larger and passes through the N stacked planes. The function $\phi(a)$ is the effective pore area distribution of the sample. It is also a mathematical model of the medium in which the important sample properties relevant to a flow situation are imbedded.

To determine the pressure drop for a given flow rate, Somerville used the equations for flow in capillary tubes for continuum, slip and free molecule flow depending on the local Kn. The equations, their derivation and the range of their validity are given by Kennard [10]. It is further assumed that there is no pressure variation through the porous medium in the transverse flow direction and that the slip flow equation is applicable to the entire transition regime. The differential equations which result from combining the flow equations with the porous carbon model are then solved numerically.

The number of planes required to simulate the porous medium, which is the only adjustable parameter in the model, is determined in the solution phase by a trial and error procedure, where the calculated pressure drop is matched with the experimental one.

The "dusty gas" model of Evans, Watson and Mason consists of regarding the porous medium as suspended dust particles constrained in space. By formally treating these particles as giant molecules, the application of kinetic theory results in a solution valid over the entire Knudsen number range. This model involves three experimental constants, one of which is the tortuosity.

In the models just described, the phenomenon of physical adsorption of the gas to the pore walls has been tacitly ignored. This problem has been subjected to many investigations and it is shown [11] that adsorption may affect both the transient and steady flow behavior in a fine-pored carbon.

2.3 A Critical Review of Available Models

The Carman and Arnell Equation (2.2) has been used to correlate porous carbon permeabilities. Nuclear grade carbons, for example, are frequently characterized by the values of B_0 and K_0 obtained from flow experiments. Although permeability is known to be very sensitive to changes in pore structure, the use of Equation (2.2) to deduce such information can lead to serious errors. Grove [12], on the basis of existing data, discusses these errors and concludes that the application of the Carman and Arnell model does not lead to a satisfactory description of the effect of gas properties on the permeability of the same carbon sample.

One important implication of this model is that once B_0 and K_0 are determined for a given sample and flow conditions, the permeability at any other mean pressure can be calculated. However, mean pressure alone does not uniquely specify the flow condition; the same p_m may be obtained either by a high inlet pressure and a large pressure drop, or by a low inlet pressure and a small pressure drop. The flow regimes encountered in the sample in these two cases may very well be different, and one would expect a corresponding change in the permeabilities. Therefore, the use of the Carman and Arnell model should be restricted to a fixed inlet or outlet pressure. Nevertheless, some investigators have found the model applicable even when the inlet pressure varied (e.g., Hutcheon, et al.,) [13]. It is plausible that in these cases, due to the distribution of pore sizes, inlet pressure variations do not effect a significant change in the flow regimes.

A major disadvantage inherent in the Carman and Arnell equation is the difficulty involved in using their model for the prediction of permeabilities. For example, there are no direct measurement methods for some of the parameters involved in B_0 and K_0 such as the tortuosity, k_t , and the shape factor, k_1 . Only by conducting flow experiments can k_t and k_1 be determined.

Somerville's model includes many advantages not present in any other model to date. A physically meaningful description of the porous medium is given and all the important flow parameters are incorporated in the gas-porous medium interaction. Different flow regimes are allowed to occur simultaneously in different

pores according to the local value of the Knudsen number. Since the entire spectrum of the mercury penetration curve is included in the description of the sample, most of the sample's relevant properties are present in the model. As a result, resort to flow experiments is required for the determination of only one parameter in the model, namely the number of stacked planes required, N . Once N is determined for a particular sample and gas, the model may be used to predict permeabilities as a function of inlet pressure, temperature gradient, and other flow parameters. Other information, such as the distribution of pressure and the fraction of flow in a given regime throughout the porous sample, may easily be determined [3].

In the "dusty gas" model of Evans, Watson and Mason, the concept of tortuosity, although subject to serious criticism, has been retained. In addition, the model involves two transport parameters which have to be determined by flow experiments. Whether or not these parameters are constants has not been fully determined.

2.4 Implications of Previous Investigations

In many instances, the factors B_0 and K_0 in the Carman and Arnell formulation have been found to be not only dependent on the porous material, but also on the gas used [12]. The nature of this dependence has not been established. In the case of Somerville's model, since all the correlations were done with a single gas (nitrogen), it is not known whether N has any relationship with the properties of the gas used.

The effect of temperature has been investigated by Hutcheon, et al., [13], but the effect of a temperature gradient in the flow direction has not been fully determined.

Whether or not mean pressure alone uniquely establishes the permeability has not been subjected to experimental determination.

The separation of gas and porous medium properties in the formulation of any model, therefore, must involve the use of gases with diverse properties and the same porous medium sample in a consistent experimental program.

CHAPTER III

EXPERIMENTAL APPARATUS AND PROCEDURE

3.1 Introduction

In the experimental determination of the isothermal permeability of a given porous carbon for a given gas, the volume flow rate, inlet pressure, and the pressure drop must be measured. If a temperature gradient is also present, the inlet and outlet carbon surface temperatures must also be known. In this chapter, the apparatus, the characteristics of the porous carbons and the gases, the experimental procedure, and the errors involved in the measurements will be discussed.

3.2 The Apparatus

The apparatus used in this study was originally designed and built by Somerville [3]. To appreciate the nature and function of the hardware involved in the experiment, it is best to follow the flow path of the gas conceptually. A schematic diagram of the overall set-up is shown in Figure 1 for this purpose.

After the gas supply pressure is adjusted with the two pressure regulators, it flows through a calibrated rotometer where the flow rate is measured. Then the gas enters the test cell where it is forced through the porous sample. The inlet pressure and the pressure drop across the sample are measured by mercury manometers. The throttle valve immediately downstream of the test cell allows the adjustment of the flow rate without affecting the inlet

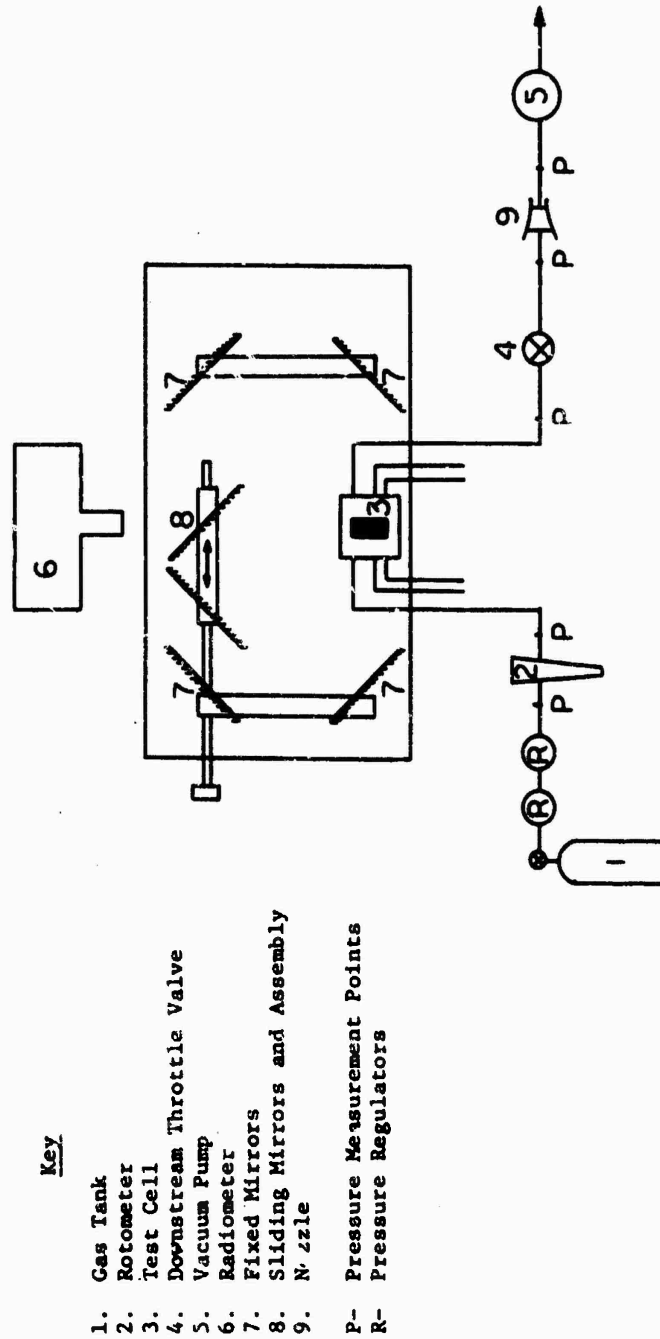
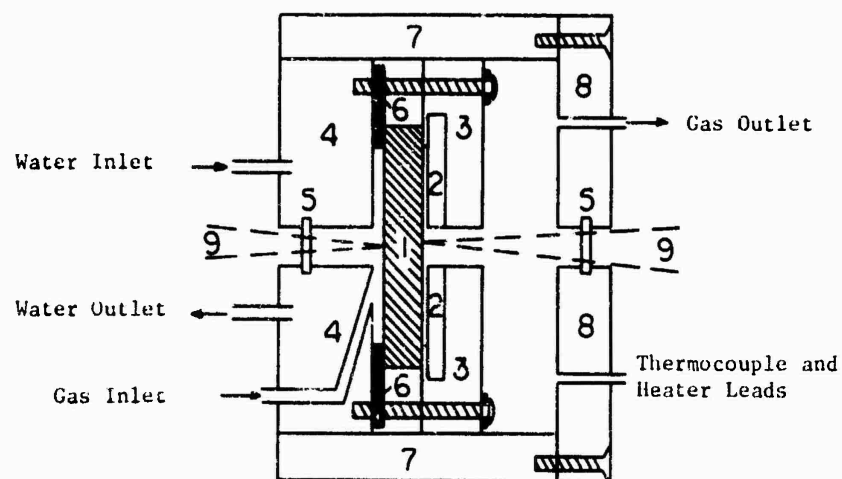


Figure 1 Schematic Diagram of Experimental Set-Up

pressure. The gas subsequently flows through a calibrated nozzle where the flow rate may be measured again. The agreement between the two flow rates, measured by the rotometer and the nozzle, indicates that the flow is steady. The gas is finally discharged to the atmosphere through the vacuum pump.

The rotometer and the nozzle were calibrated for all the gases involved in the experiment by using a water displacement technique. To determine the temperature gradient, the temperatures of the carbon on the inlet and outlet surfaces were measured by the combination of a radiometer, and four fixed and two sliding front-surfaced mirrors. The temperature gradient was imposed by a disk-shaped electric heater on the hot side, and an aluminum water jacket on the cold side of the porous carbon sample. The constructional details of the test cell are shown in Figure 2. The sodium chloride crystal windows which are mounted on the body of the cell allow the passage of the radiation from the sample surface to the mirrors. The sliding mirrors allow the radiometer to view the two sides of the porous carbon. A thermocouple was buried in the hot surface of the carbon. The temperature indicated by this thermocouple provided a check on the radiometer reading. Two other thermocouples, one on the heater surface and the other on the water-cooled jacket were also installed. A photograph of the assembly is given by Somerville [3].

Two rotometers consisting of Matheson tubes 600 and 601 with dual floats were used throughout the experiments. The nozzle was built of sapphire by Richard H. Bird and Company with a throat



Key

- | | |
|----------------------------|----------------------------|
| 1. Porous Carbon Sample | 6. Rubber Gasket |
| 2. Heater | 7. Test Cell Body |
| 3. Heater Assembly | 8. Sealing Head |
| 4. Water-Cooled Jacket | 9. Radiometer Viewing Path |
| 5. Sodium Chloride Windows | |

Figure 2 Test Cell Components

diameter of 0.015 inch. The radiometer was the 8RT1 model manufactured by Barnes Engineering Company, and it was calibrated with a black body reference source. The calibration incorporated the mirrors and the sodium chloride windows which were present in actual carbon surface temperature measurements. All thermocouple junctions were made of 0.005-inch chromel and alumel wires with glass insulation.

3.3 The Porous Samples

Two different porous carbons were used in this investigation. They are both fuel cell grade carbons, denoted by the prefix "FC." They are identified as FC-01 and FC-25 by Pure Carbon Company, the supplier. Each sample was machined into a disk 2 3/4 inches in diameter and 1/2 inch in thickness. To assure that flow occurred only in the axial direction, the samples had to be sealed radially around the periphery of the disks. This was accomplished by cementing a ceramic ring, 0.125 inch in thickness, to the sample. On the cold side of the carbon, a layer of epoxy was added between the sample and the ring to assure that no flow would occur in the cement. Subsequently, the samples were glued to a rubber gasket. This procedure resulted in a cross sectional flow area of 4.91 squared inches on the sample. The resulting sample assembly was then sandwiched between the heater and the water-cooled jacket by tightly screwing the heater to the jacket with the sample assembly in between as shown in Figure 2.

Micrometrics Instrument Corporation performed mercury porosimetry tests on smaller carbon samples of FC-01 and FC-25

which were obtained from the same block of carbons from which the test samples were machined. The resulting mercury penetration curves are shown in Figures 3 and 4.

3.4 The Gases

Four gases were chosen for the experimental investigation. These are helium, nitrogen, argon and sulfur hexafluoride. They cover a wide range of molecular weights and viscosities and are all inert and non-toxic at ordinary temperatures. Some of the properties of these gases at a temperature of 288°K are given in Table 1.

Table 1

Properties of the Gases Used in the Investigation

Gas	Molecular Weight	Viscosity x 10 ⁶ gm/cm-sec	Mean Free Path x 10 ⁶ cm
Helium	4	194	18.62
Nitrogen	28	173	6.28
Argon	40	220	6.66
Sulfur Hexafluoride	146	149	2.42

Helium, nitrogen and argon are well-known ideal gases at the pressures and temperatures encountered in this investigation.

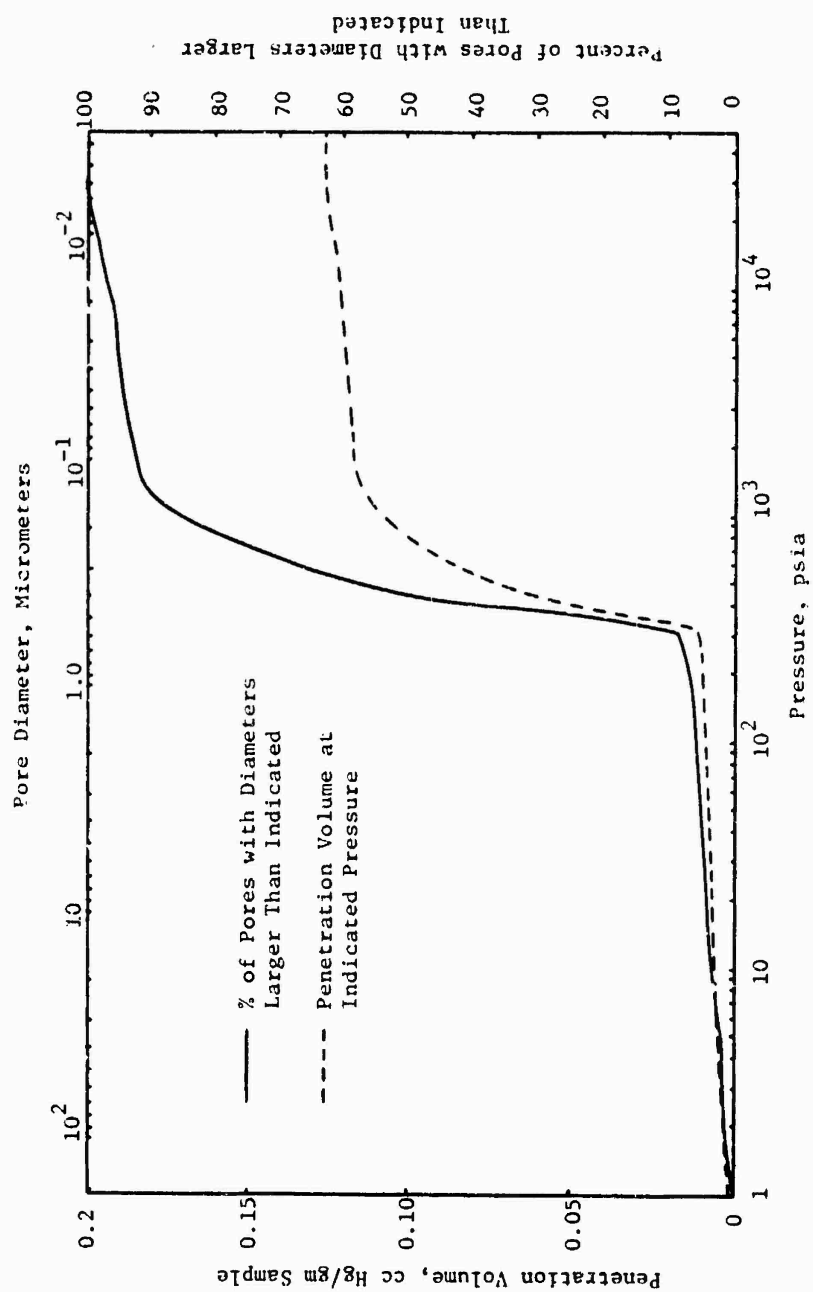


Figure 3 Results of the Mercury Porosimetry Test for FC-01

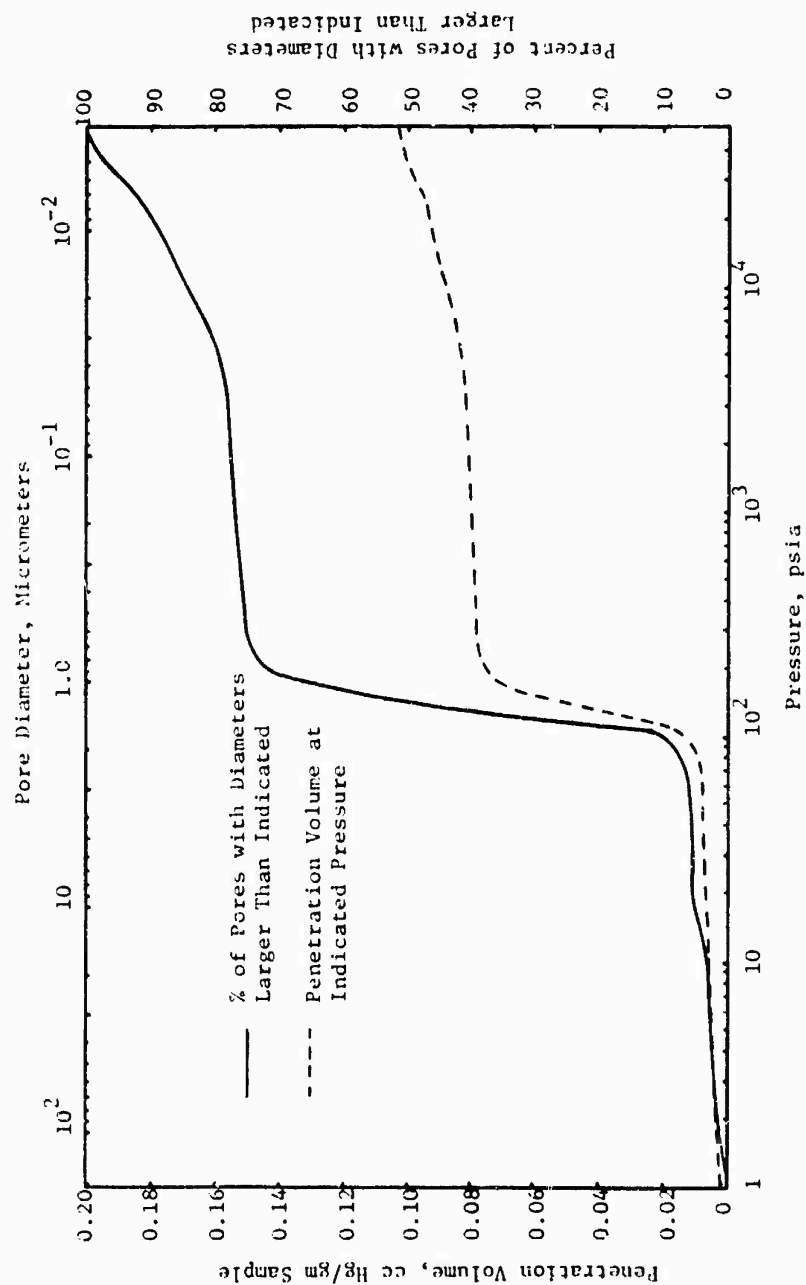


Figure 4 Results of the Mercury Porosimetry Test for FC-25

The compressibility factor, Z , for sulfur hexafluoride, given by

$$Z = \frac{pM}{\rho RT} \quad (3.1)$$

has a value of 0.981 at a pressure of 1 atm. and a temperature of 298°K. Therefore, the error involved in using the ideal gas equation of state in determining the density of this gas under these conditions is less than 2%.

3.5 Experimental Procedure

Before the actual flow tests were executed, the two samples were tested for radial leakage. At the highest pressure drop encountered during the flow tests no radial leakage was observed. A typical experiment consisted of installing the sample assembly in the test cell as shown in Figure 2. The test cell was then closed and the inlet and outlet tubes were connected. The entire system was then evacuated to a pressure of about 4 in. Hg absolute by starting the vacuum pump, closing the valve upstream of the rotometer and opening the downstream throttle valve. The system was kept under an evacuated condition for about one hour to assure the desorption of foreign gases from the porous carbon. Gas was then admitted to the system. The heater voltage and the flow rate of cold water in the jacket were adjusted, and the inlet pressure was fixed at 30 in. Hg absolute. The system was allowed to run at the highest gas flow rate until steady flow was achieved. The pressure drop across the sample, the flow rate, and the hot and cold carbon surface temperatures were then recorded. This measurement procedure was repeated for the

same inlet pressure and temperature conditions of the sample under different flow rates. At each flow rate setting, which was accomplished by the adjustment of the downstream throttle valve, the system was allowed to reach steady state.

The entire procedure outlined above was repeated for the four gases and the two carbon samples. Except for sulfur hexafluoride, each gas was run under zero, positive and negative temperature gradient conditions. The negative temperature gradient was achieved by simply reversing the direction of the flow through the test cell. Due to the uncertainty regarding the chemical stability of sulfur hexafluoride at high temperatures, positive and negative temperature gradient conditions were not attempted for this gas.

3.6 Measurement Errors

Considering the instrumentation and the reproducibility of data in the calibration of the rotometers and the radiometer, the certainty regarding the measured parameters may be estimated. The errors involved in the flow rate measurements by the rotometer are twofold. One involves the reproducibility of data which was determined during calibration, while the other involves the accuracy with which the position of the floats in the flowmeter tubes can be read. Thus, in the case of the flow of argon in the Matheson 600 tube, at a flow rate of 40 standard cc/min, the error involved in reading the position of the floats leads to an uncertainty which is less than 0.3 standard cc/min in the flow rate. At flow rates about 5 standard cc/min, this uncertainty decreases to about 0.2

standard cc/min. The reproducibility of calibration points was found to be excellent in both high and low flow rates.

The uncertainties in the measurement of temperature by the radiometer are of a more complex nature. These include the assumption that the emissivity of the carbon surfaces in the test cell is unity. Moreover, errors are involved in the reduction of radiometer data from the net voltage output of the radiometer electronics unit to a final value for the temperature. This procedure is outlined in detail by Somerville [3]. By considering all the factors involved, the temperature measurements are estimated to be within 2% of their true values on the Kelvin scale.

Since all the crucial pressure measurements were taken from mercury manometers, the only error which may be of significance is the readability of the level of mercury. The resulting error is within 0.1 in. Hg.

CHAPTER IV

EXPERIMENTAL RESULTS

The inlet pressure for all the flow experiments was kept constant at 30 in. Hg absolute. At room temperature, therefore, the inlet volume flow rate, Q_{in} , which is measured on the upstream side of the carbon sample, and the pressure drop, Δp , uniquely determine the permeability for a given gas. Assuming that the densities of all the gases are given by the ideal gas relation

$$\rho = \frac{pM}{RT} , \quad (4.1)$$

the mass flow rate can be easily determined as follows:

$$\dot{m} = \rho_{in} Q_{in} . \quad (4.2)$$

For the FC-01 carbon, the mass flow rate of argon as a function of the pressure drop, under zero, positive and negative temperature gradient conditions is shown in Figure 5. Even though this carbon sample has very fine pores, and the free molecule flow regime is expected to occur through most of the sample, the temperature gradient itself did not seem to affect the flow. This is evidenced by the coincidence of the positive and negative temperature gradient flow values in Figure 5. This effect was observed in the results of all the flow experiments. The observed decrease in the mass flow rate in the presence of a temperature gradient is totally attributed to the dependence of gas properties on temperature in that

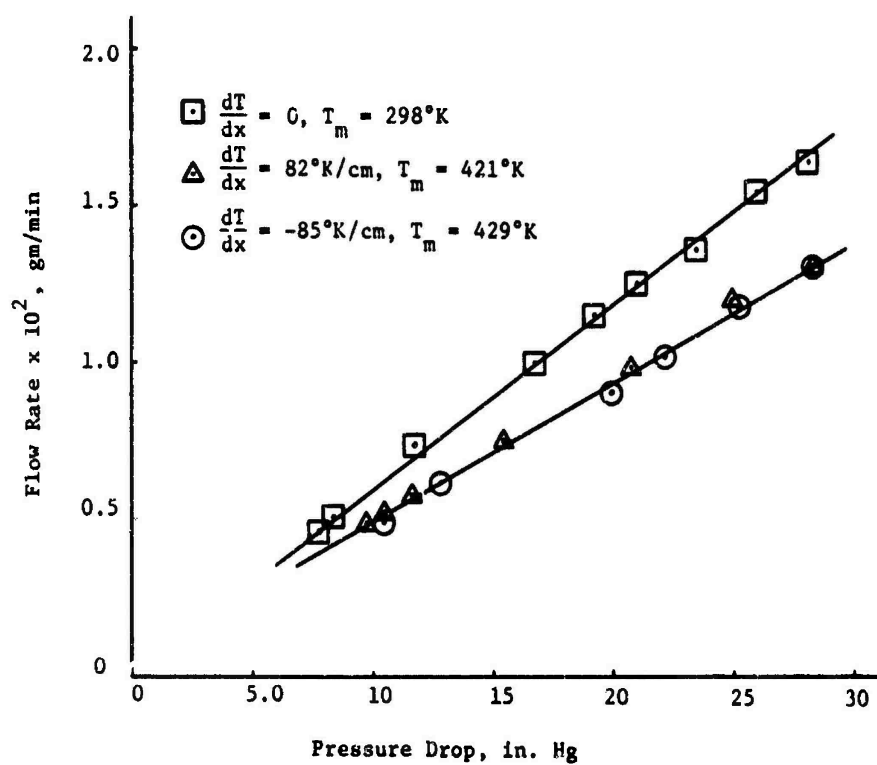


Figure 5 Mass Flow Rate of Argon in FC-01 Versus Pressure Drop

a mean temperature increase reduces the density and increases the viscosity of the gas.

The lack of an observable effect due to the temperature gradient is predictable. Even if free molecule flow is the dominant flow regime in these carbons, the flow rates due to the pressure drops are so high that the contribution of thermal diffusion becomes negligible.

In flow studies through porous media, it is customary to present the data in the form of permeability, K , as a function of mean pressure, P_m . From the definition of permeability in Equation (2.1) and the value of the inlet pressure, such a graph is easily obtainable from the experimentally measured parameters. For the flow of argon in FC-01, this is shown in Figure 6.

The existence of a permeability which is independent of the mean pressure, as in the present case, is evidence that free molecule flow is the dominant flow regime. In general, if the inlet pressure is kept constant, the shape of the permeability versus mean pressure curve indicates the flow regime which has the most influence on the gross characteristics of the flow. These are discussed in detail by Grove [12].

For the flow of argon in FC-25, mass flow rate as a function of pressure drop, and permeability as a function of mean pressure are shown in Figures 7 and 8, respectively. Due to the existence of larger pores in FC-25, for a given pressure drop the flow rates are higher than those in FC-01. A corresponding increase in the permeability is also observed. As before, temperature gradient

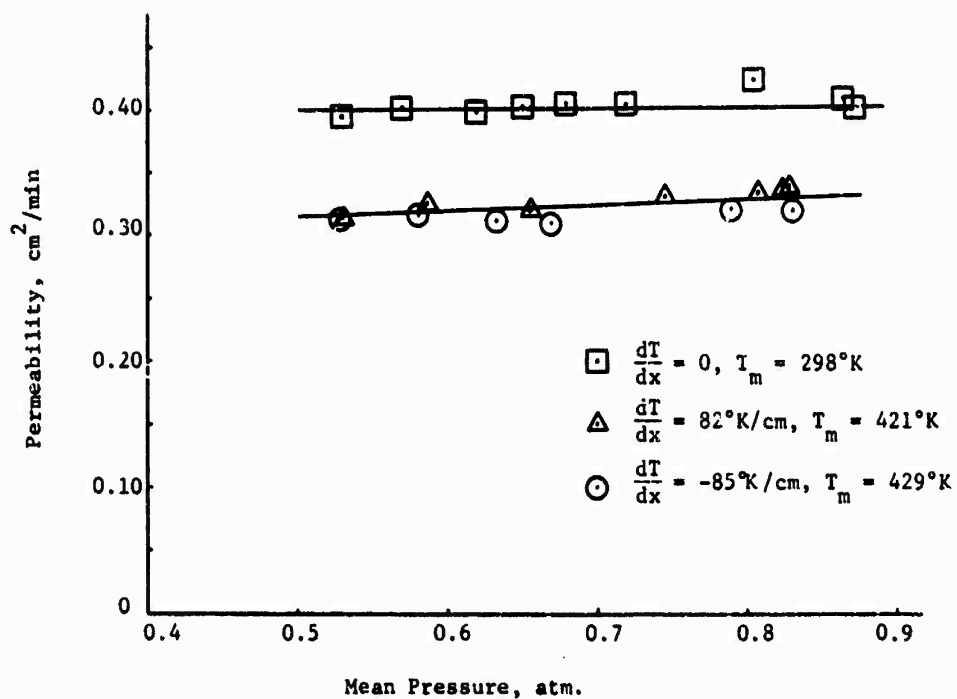


Figure 6 Permeability Versus Mean Pressure for Flow of Argon in FC-01

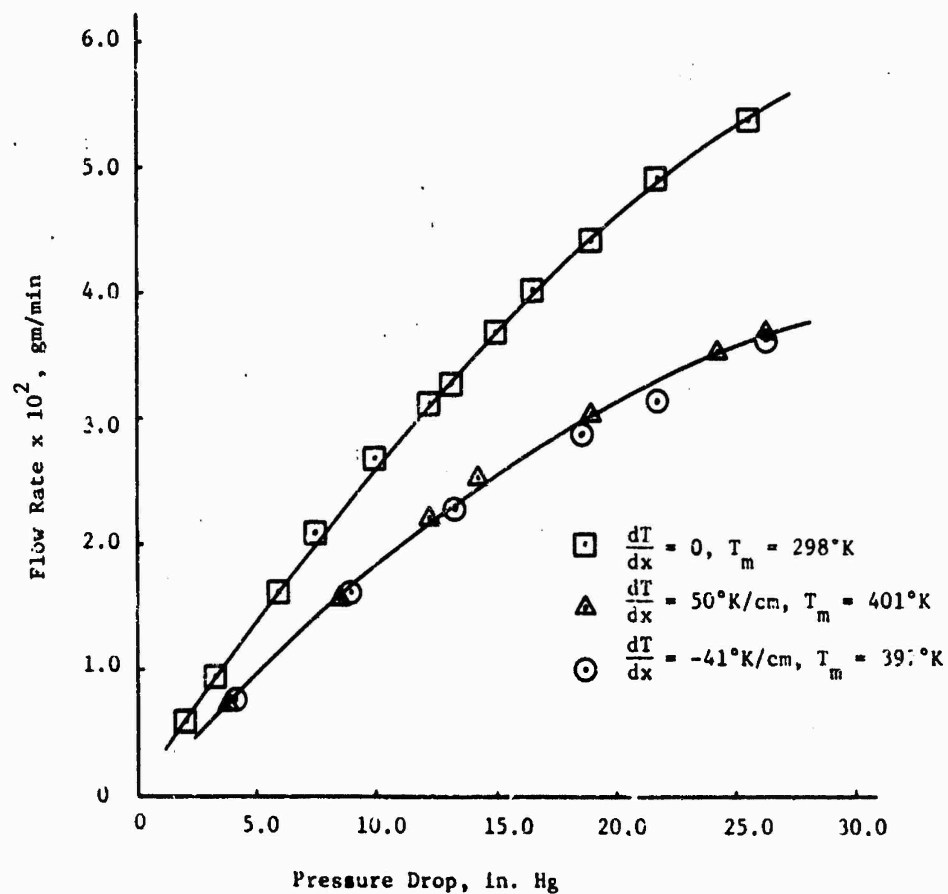


Figure 7 Mass Flow Rate of Argon in FC-25 Versus Pressure Drop

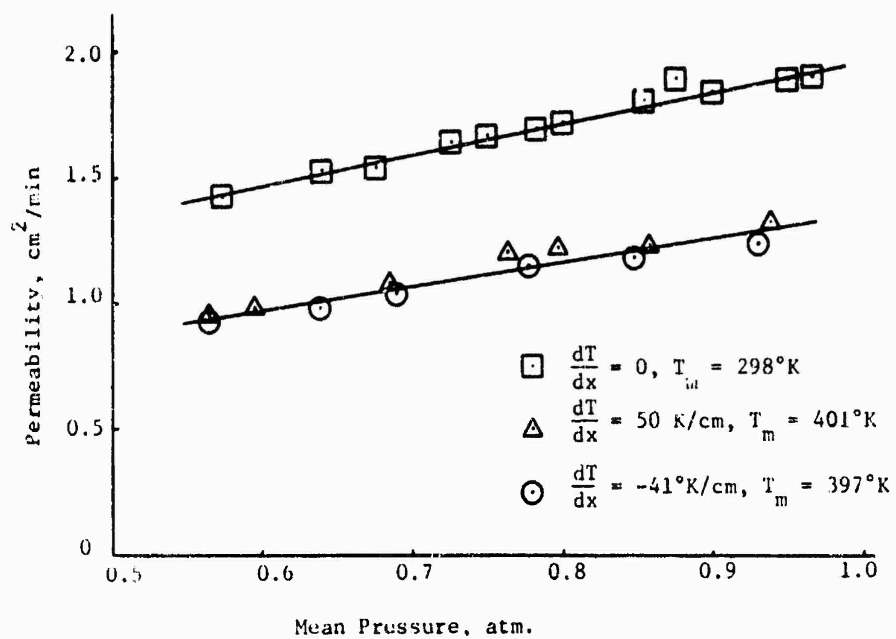


Figure 8 Permeability Versus Mean Pressure for Flow of Argon in FC-25

itself does not have any appreciable effect on the flow. In contrast with flow in FC-01, permeabilities show a definite rise with mean pressure increase, indicating the influence of continuum flow.

The flow characteristics of argon in the two carbons are more or less typical of those of the other gases examined, as evidenced by the flow rate versus pressure drop curves in Figure 9 for the FC-25 carbon. The reduced experimental data for all the flow experiments (helium, nitrogen, argon and sulfur hexafluoride) are presented in the Appendix.

The isothermal permeabilities for the flow of all the gases through FC-01 and FC-25 are shown in Figures 10 and 11, respectively. In the case of the flow of nitrogen in FC-01, Somerville [3] reports a permeability which rises with the mean pressure increase. Since he conducted his experiments under varying inlet pressure conditions, it is concluded that mean pressure alone does not uniquely define the permeability. This conclusion is consistent with the observation that different flow regimes may exist with the same mean pressure. Thus, the observed rise in the permeability in the case of Somerville's data is totally attributed to inlet pressure variations.

At a mean pressure of 0.7 atm. and room temperature, the viscosities, molecular weights and the Knudsen numbers based on the median pore diameters of the two carbons are given in Table 2. By noting that the important gas parameter for high Knudsen number flows is the viscosity, and for low Knudsen number flows is the molecular weight, the qualitative behavior of the gases in the two porous carbons as shown in Figures 10 and 11 can be appreciated.

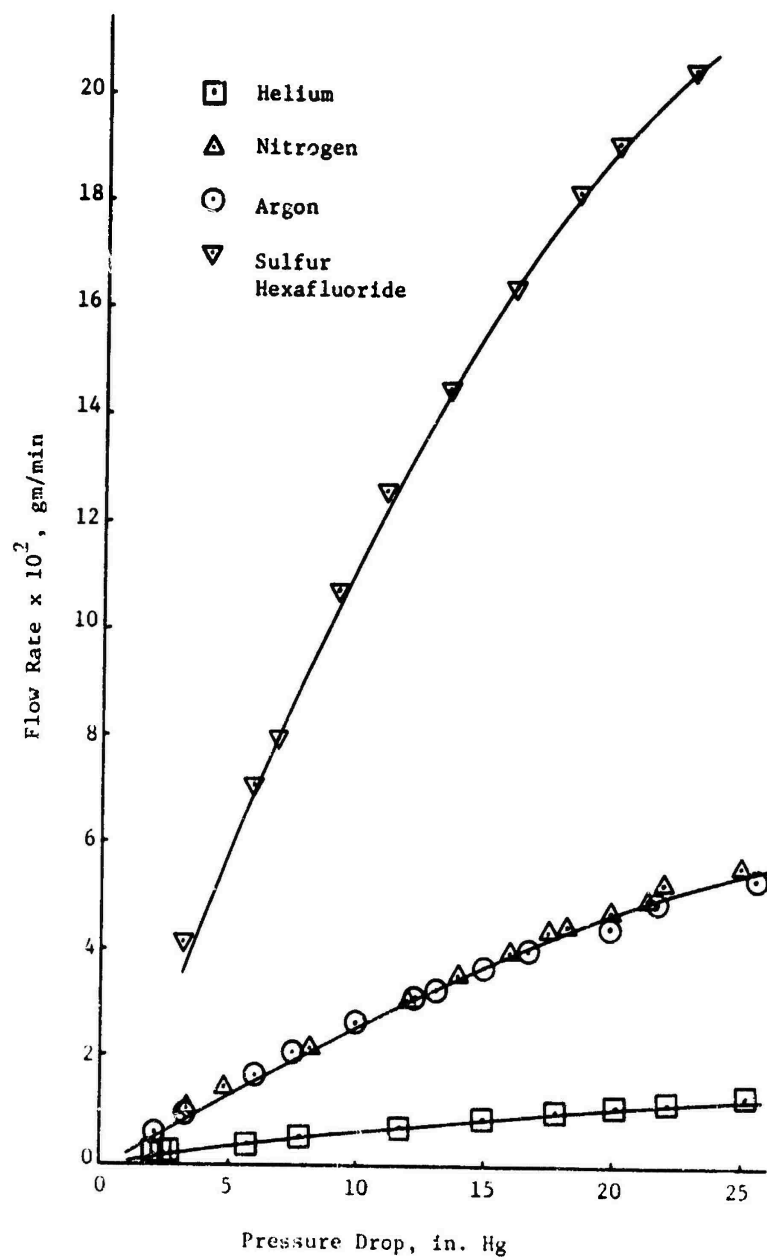


Figure 9 Isothermal Mass Flow Rates Versus Pressure Drop in FC-25

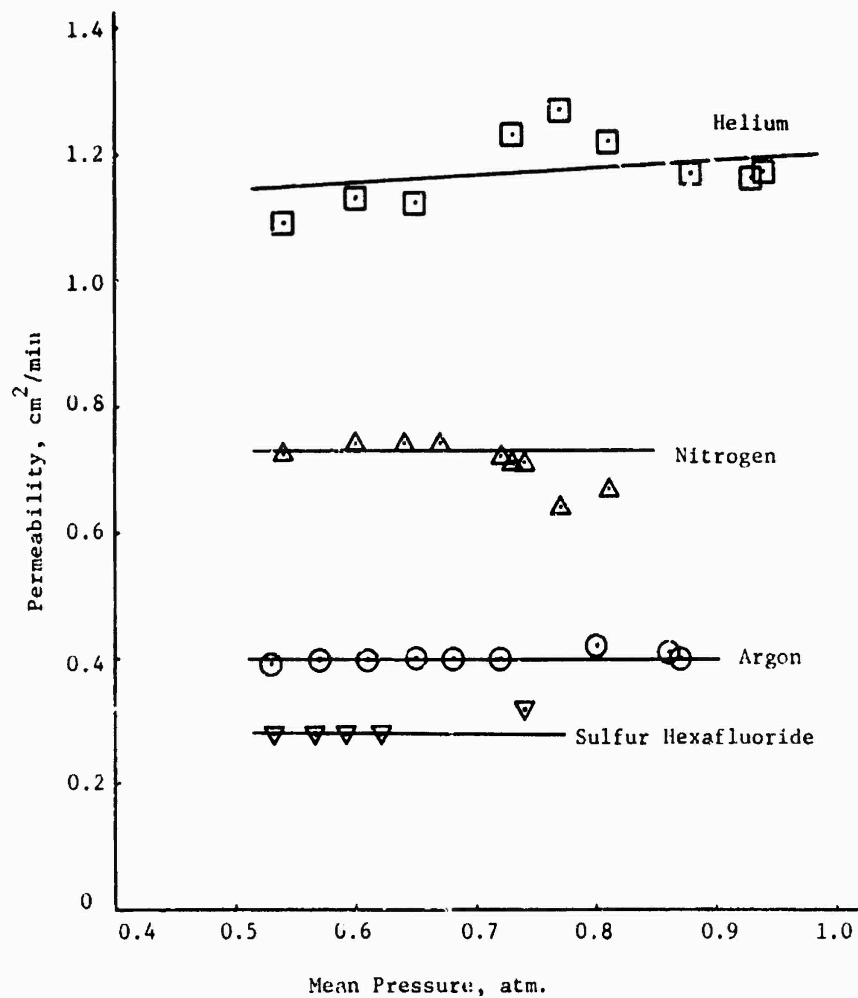


Figure 10 Permeability Versus Mean Pressure in FC-01

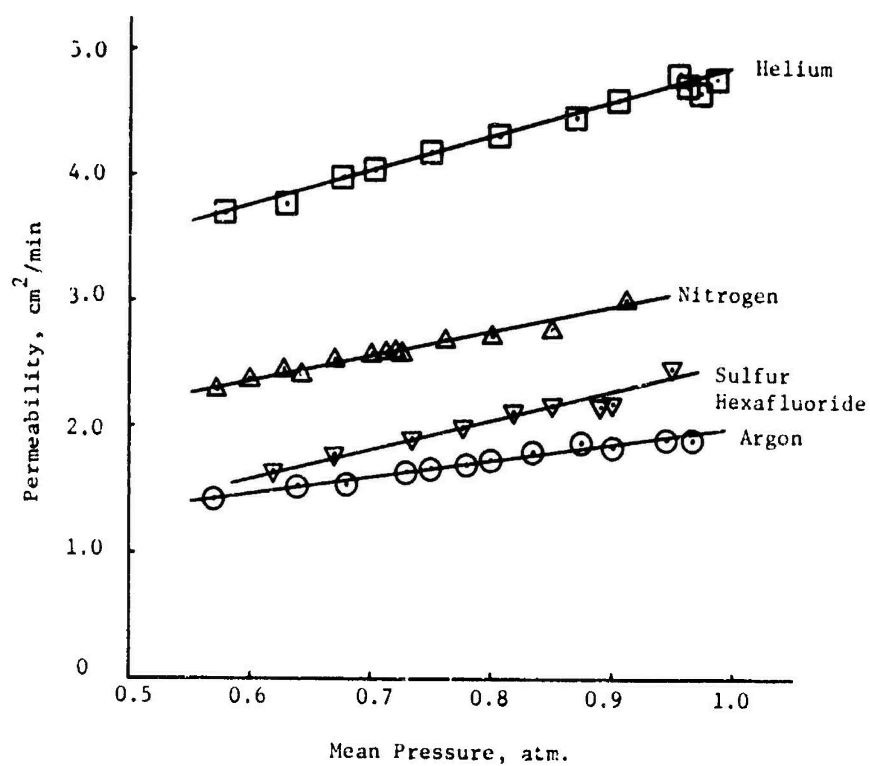


Figure 11 Permeability Versus Mean Pressure in FC-25

The FC-01 permeabilities increase with decreasing molecular weights, further verifying the dominance of free molecular phenomena. The relative shift of the argon and sulfur hexafluoride permeabilities in FC-25 clearly indicates the influence of the low viscosity of the latter, signifying the relative importance of continuum phenomena.

Table 2

Significant Gas Parameters in Flow Through FC-01 and FC-25
at Room Temperature and 0.7 atm. Pressure

Gas	Molecular Weight	Viscosity x 10 ⁶ gm/cm-sec	Knudsen Number	
			FC-01	FC-25
Helium	4	194	1.40	4.62
Nitrogen	28	173	4.02	13.20
Argon	40	220	3.90	12.80
Sulfur Hexafluoride	146	149	10.70	35.10

A detailed examination of the effect of gas properties on the permeability of FC-01 and FC-25 is the subject of the next chapter.

CHAPTER V

DEPENDENCE OF PERMEABILITY ON GAS PROPERTIES

5.1 Introduction

Permeability is a measure of the flow rate per unit sample area per unit pressure gradient. It is not a porous medium property. As a result, the thermodynamic and transport properties of the gas and some unknown properties of the porous carbon all constitute the variables on which permeability depends. The determination of the relationship between the gas properties and the permeability will be discussed in this chapter.

5.2 Application of Existing Models

The most widely used model in permeability determinations is the one developed by Carman and Arnell and given as

$$K = \frac{B_o}{\eta} p_m + \frac{4}{3} K_o \bar{v} . \quad (2.2)$$

On a permeability versus mean pressure curve, $\frac{B_o}{\eta}$ is the slope and $\frac{4}{3} K_o \bar{v}$ is the K-intercept. As pointed out in Chapter II, B_o and K_o are, presumably, porous medium properties alone. The success of the model lies in the accuracy with which experimentally determined values of B_o and K_o for one gas may be used to predict permeabilities for other gases.

These two parameters were calculated from experimentally determined isothermal permeabilities for helium, nitrogen, argon and sulfur hexafluoride in FC-01 and FC-25. These values are given in Tables 3 and 4. Hutcheon, et al., [13], working with fine-pored

Table 3

Values of B_0 and K_0 for FC-01

Gas	B_0, cm^2	K_0, cm
Helium	5.7×10^{-13}	1.05×10^{-7}
Nitrogen	0	1.92×10^{-7}
Argon	0	1.28×10^{-7}
Sulfur Hexafluoride	0	1.66×10^{-7}

Table 4

Values of B_0 and K_0 For FC-25

Gas	B_0, cm^2	K_0, cm
Helium	8.48×10^{-12}	2.11×10^{-7}
Nitrogen	5.68×10^{-12}	3.14×10^{-7}
Argon	4.58×10^{-12}	2.21×10^{-7}
Sulfur Hexafluoride	5.53×10^{-12}	1.93×10^{-7}

carbons, calculated the values for B_0 and K_0 from flow data. Their reported numbers are of the same order of magnitude as those in Tables 3 and 4. For the present study, although the order of magnitude of B_0 's and K_0 's are the same for a given carbon, in some cases, there is significant variation from gas to gas. Thus, the present results imply that characterization of fine-pored carbons by B_0 and K_0 alone is not adequate. In cases where variations of these parameters are observed depending on which gas is used, their relationship with the gas properties is not known.

In the application of Somerville's model [3], the only parameter to be determined experimentally is the number of zero thickness planes that need to be stacked, one behind the other, to obtain the experimentally observed pressure drop for a given rate of flow. These numbers were determined by a trial and error procedure from Somerville's computer solution and are given in Table 5 for flow in FC-25.

Table 5

Values of N Using Somerville's Model for FC-25

Gas	Helium	Nitrogen	Argon	Sulfur Hexafluoride
N	15.5	13.0	14.5	13.5

Contrary to Somerville's findings, permeability was found to be a highly sensitive function of N . In the light of this observation, although the values of N given in Table 5 are not too far apart the use of the same N to predict permeabilities for different gases can lead to seriously erroneous results. For example, in the case of flow of argon in FC-25, an increase of 3.4% in N in the computer solution decreases the predicted permeability by as much as 7.4%. Thus, N is also dependent on the gas used. However, after this parameter is determined for a given gas and porous material, it can be successfully used to predict the permeability under different flow conditions.

5.3 A New Experimental Correlation

The complex structure of consolidated fine-pored carbons can, in general, support continuum, transition and free molecule flow simultaneously. As evidenced from the permeability results given in Figures 10 and 11, the predominant flow regimes in FC-01 and FC-25 carbons can, at best, be classified as transition flows. Although the exact determination of the functional relationship between the gas properties and the permeability is a matter of considerable difficulty, some physical and intuitive arguments as to the expected nature of this dependence may be of value.

In the transition regime, the frequency of molecular collision is of the same order of magnitude as that of molecule-wall collisions. Thus, apart from the thermodynamic properties, the viscosity and the mean thermal speed become the two interacting gas parameters on which the permeability should depend. In the

limit of high Knudsen numbers, the higher the viscosity, the lower the permeability. For very low Knudsen numbers, viscosity is not important and one would expect the permeability to be a monotonically increasing function of \bar{v} .

At a mean pressure of 0.7 atm. and room temperature, the viscosities, mean molecular speeds, permeabilities and the Knudsen numbers based on the median pore diameters of the two carbons are given in Table 6. Examination of the gas and flow parameters given in Table 6 for the two carbons and the four gases can lead to a better physical understanding of the flow. For flow in the FC-01 carbon, due to the small Knudsen numbers, the free molecular regime is expected to be more predominant. This conclusion is further verified by the fact that the permeabilities increase with increasing mean molecular speeds. However, the permeabilities are not directly proportional to \bar{v} as one would expect in a purely free molecular flow. The lack of this proportionality is attributed to the variations in the viscosities of the four gases, indicating the simultaneous presence of continuum phenomena. In the case of the FC-25 carbon, due to the larger Knudsen numbers, the influence of continuum effects is more pronounced. For helium, nitrogen and argon the permeabilities increase with increasing mean molecular speeds. However, the permeability of FC-25 to sulfur hexafluoride does not follow this trend. This effect is clearly due to the low viscosity of this gas. Thus, the flow of helium, nitrogen, argon and sulfur hexafluoride is best characterized as transition flow in both porous carbons, and \bar{v} and η both have a significant influence on the permeability.

Table 6

Significant Gas and Flow Parameters

Gas	Viscosity $\times 10^6$ gm/cm-sec	Mean Molecular Speed $\times 10^{-2}$ cm/sec	Permeability cm ² /min		Knudsen Number	
			FC-01	FC-25	FC-01	FC-25
Helium	194	1245	1.18	4.00	1.40	4.62
Nitrogen	173	471	0.73	2.60	4.02	13.20
Argon	220	394	0.40	1.60	3.90	12.80
Sulfur Hexafluoride	149	206	0.28	1.80	10.70	35.10

The physical phenomena just described also suggest a technique for correlating the experimental permeabilities as a function of the gas properties. In all cases, increasing the viscosity decreases the permeability, while increasing the mean molecular speed increases the permeability. This observation suggests that the product of K , η and \bar{v} would probably correlate with a significant gas parameter, such as the molecular weight. However, instead of dealing with the product $\eta\bar{v}$, consider the mean free path, λ_m , evaluated at the inlet pressure and the mean temperature. For a hard sphere molecular model, λ_m is given by

$$\lambda_m = \frac{\eta}{P_{in}} \left(\frac{\pi RT_{in}}{2M} \right)^{1/2} = \frac{\pi}{4P_{in}} \eta \bar{v} \quad (5.1)$$

In addition to containing the two parameters, η and \bar{v} , the mean free path is inversely proportional to the Knudsen number [Equation (1.1)] which is of direct significance in flow through fine-pored media. Thus, it is expected that $\lambda_m K$ will correlate with the molecular weights of the gases.

For flow in FC-25, a log-log plot of $\lambda_m K$ versus the molecular weights of helium, nitrogen, argon and sulfur hexafluoride is shown in Figure 12. The points shown correspond to a mean pressure of 0.6 and 0.9 atm. for zero, positive, and negative temperature gradients. Since the points for a given mean pressure appear to fall on a straight line, it can be inferred that

$$K = \frac{A_0}{\lambda_m} M^\alpha \quad (5.2)$$

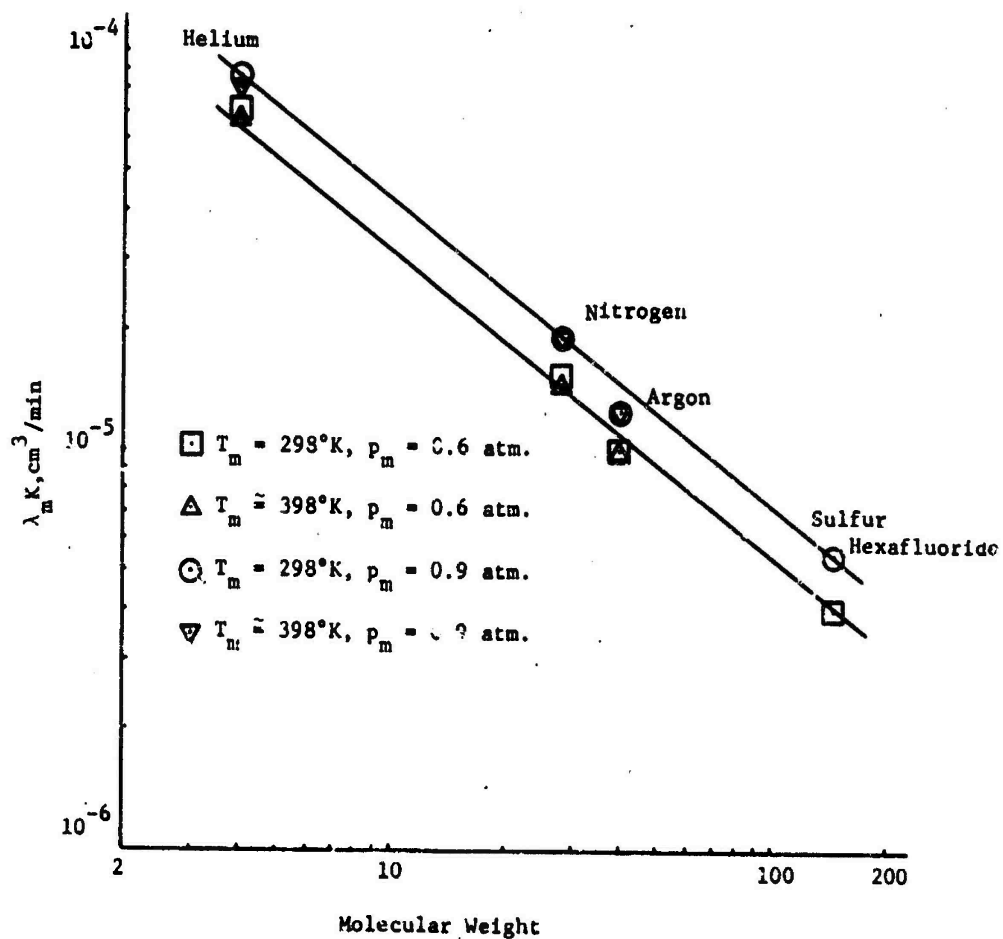


Figure 12 $\lambda_m K$ Versus Molecular Weight for FC-25

where A_0 is a function of the carbon and the mean pressure, while α is porous carbon dependent only. It is further indicated that the effect of temperature can be easily taken into account by a mean temperature correction in the λ_m term.

A similar curve for flow in FC-01 is given in Figure 13. Since mean pressure does not have a significant effect on the permeabilities, all the experimental points of Figure 10 collapse on the same point in Figure 13. Unlike the flows in FC-25, a mean temperature rise increases $\lambda_m K$ for the same gas in FC-01. Since FC-01 is a particularly fine-pored sample of graphite structure, this effect could be due to the blockage of pores as a result of adsorption. The same phenomenon, if it is in fact present, can explain the unexpectedly low $\lambda_m K$ for sulfur hexafluoride. Due to larger molecular size of sulfur hexafluoride, the blockage of pores due to its adsorption is more appreciable.

Table 7 gives the resulting values of A_0 and α for the two carbons. The value of A_0 for FC-25, as noted in the table, is not only a function of the mean pressure, but is also dependent on the pressure and temperature conditions chosen for λ_m . The exponent α , however, seems to be a function of the porous material alone, irrespective of the pressure and temperature conditions. Hence, it is expected that the permeability of any other gas in FC-01 and FC-25, under conditions not too far removed from those given in Figures 12 and 13, may be calculated from the A_0 's and α 's given in Table 7.

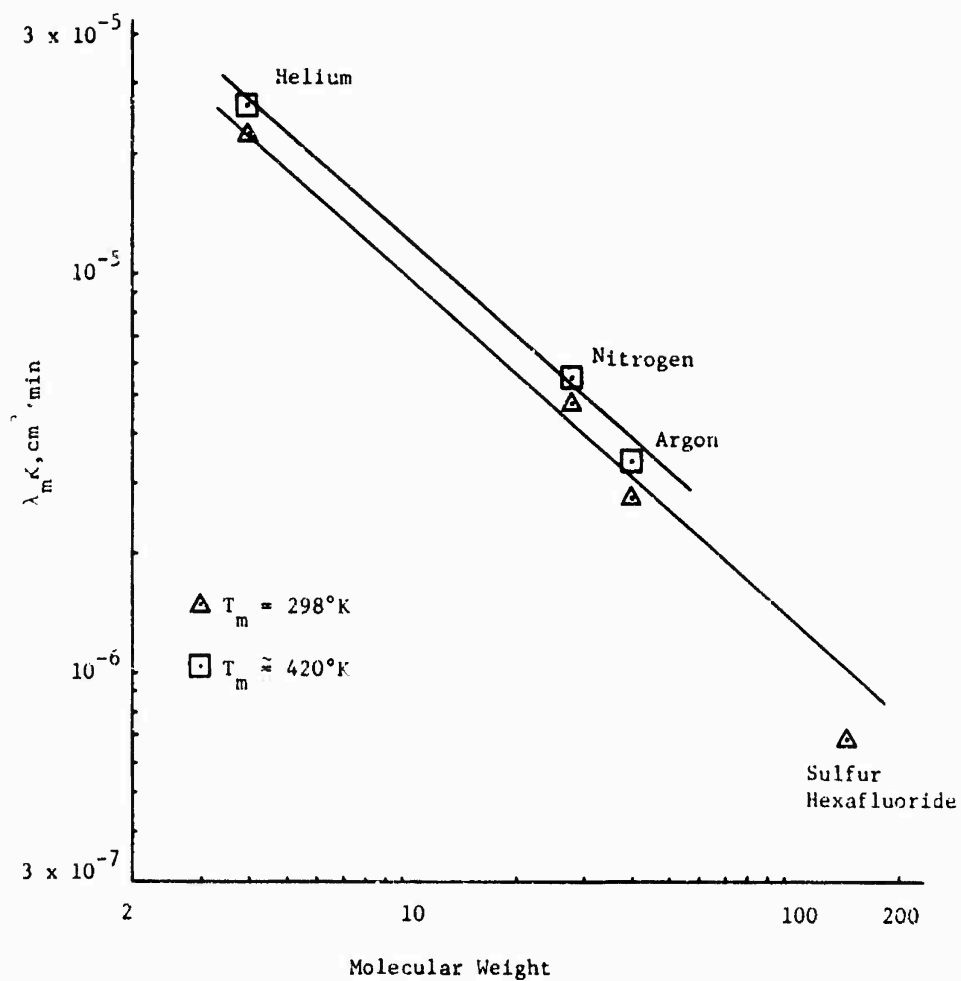


Figure 13 λ_m Versus Molecular Weight for FC-01

Table 7

Values of A_0 and α for FC-01 and FC-25 Carbons

Carbon	A_0 , cc/min		α
	$p_m = 0.6$	$p_m = 0.9$	
FC-01	7.2×10^{-5}	7.2×10^{-5}	-0.86
FC-25	1.94×10^{-4}	2.48×10^{-4}	-0.77

5.4 Proposed Correlation Applied to Other Data

Barrer and Strathan [11] report their experimentally determined permeabilities for the flow of hydrogen, helium, nitrogen, neon, argon and krypton in compacted Carbolac carbon powder at low pressures, under isothermal conditions at 298°K. Their reported permeabilities do not show a significant variation with the mean pressure, indicating the influence of free molecular phenomena. The application of the Carman and Arnell equation

$$K = \frac{B_0}{\eta} p_m + \frac{4}{3} K_0 \bar{v} \quad (2.2)$$

implies that $B_0 = 0$. Thus, it is expected that a plot of K versus \bar{v} for all the gases involved would result in a straight line, with $\frac{4}{3} K_0$ as the slope. Such a plot is shown in Figure 14. This figure implies that no matter how K_0 is related to the more familiar porous medium properties, it is also dependent on the gas. Thus, the Carman and Arnell model, although applicable under certain circumstances, fails in this case also.

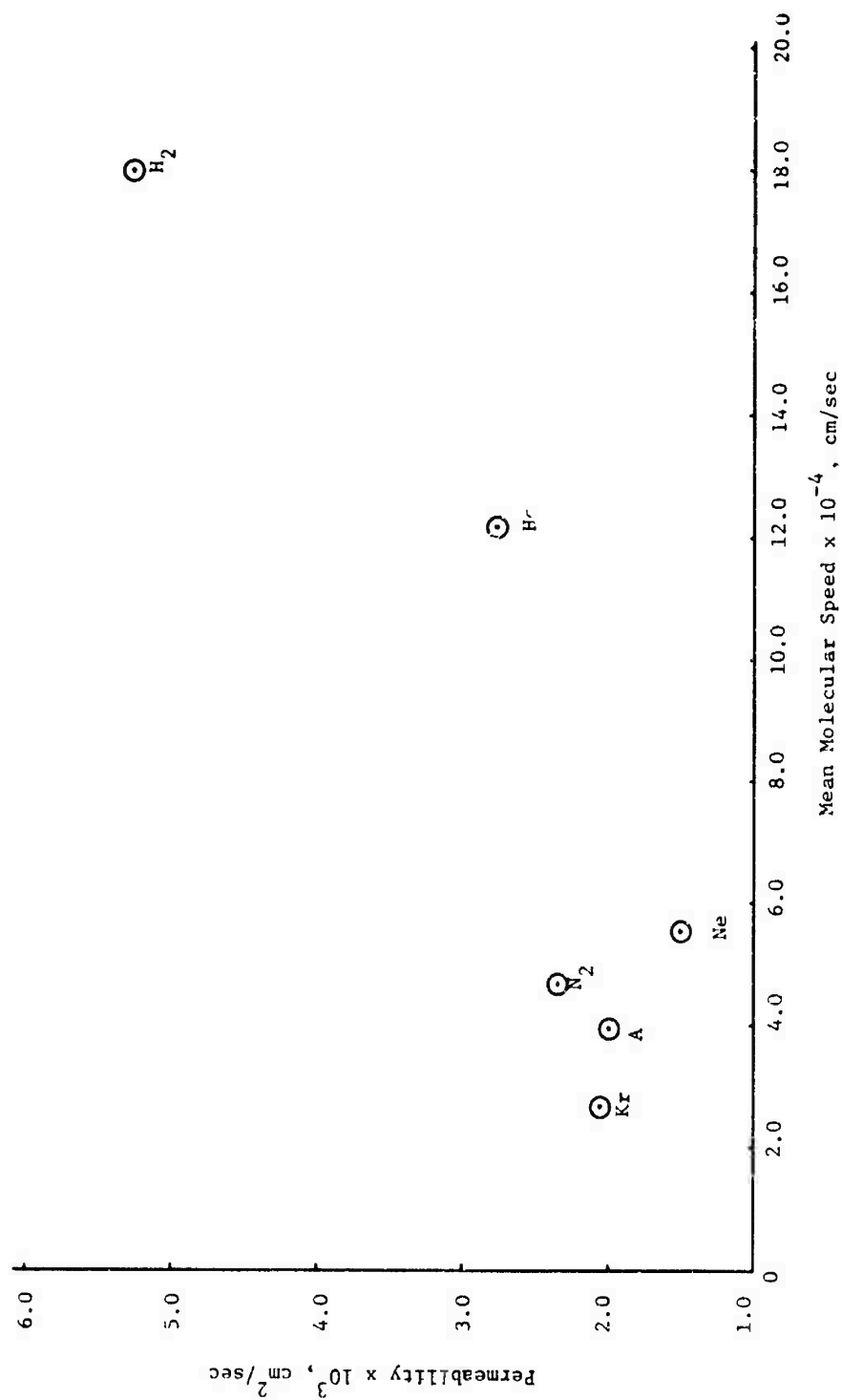


Figure 14 Permeability Versus Mean Molecular Speed, from
Barrer and Strachan's Data [11]

As a test of the newly-proposed experimental correlation given in Equation (5.2), a plot of the product of the mean free paths and the permeabilities versus the molecular weights of the gases is shown in Figure 15. The mean free paths chosen in this case are those at atmospheric pressure and 298°K. The choice of the atmospheric pressure instead of the actual inlet pressure (not known) has the sole effect of altering the value of A_0 , leaving α unchanged. On the basis of this correlation, all the experimental points are predictable with an accuracy higher than 12%. Since the gases involved in Barrer and Strachan's experiments possess diverse physical properties, the success of the present correlation implies that the important gas and porous medium parameters have been distinguished from each other in Equation (5.2), and that this equation adequately expresses the effect of gas properties on the permeability of fine-pored carbons.

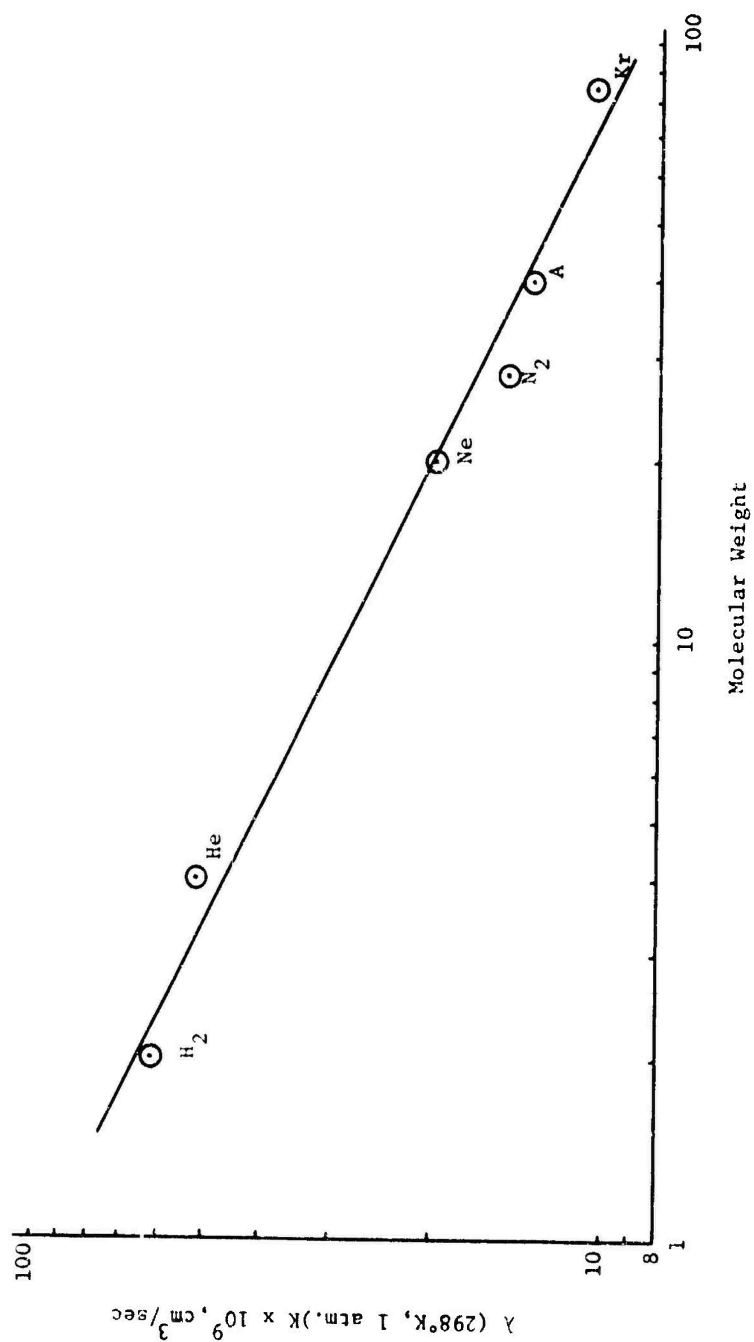


Figure 15 λ (298°K , 1 atm.) K Versus Molecular Weight, from Barrer and Strachan's Data [11]

CHAPTER VI

SUMMARY AND CONCLUSION

6.1 Summary

An experimental investigation of the permeability of two fuel cell grade fine-pored carbons with four gases of diverse physical properties has been presented in the previous chapters. The determination of the effect of gas properties on the permeability, which was the objective of this research effort, was discussed in Chapter V. The examination of two existing mathematical models regarding gaseous flow through porous media indicated the inadequacy of these models in predicting the effect of gas properties on the permeability. A new experimental correlation which was mainly based on physical and intuitive considerations was presented. This correlation could predict permeabilities as a function of the gas properties within 7% of their true value, except in the case of the flow of sulfur hexafluoride in the finer-pored carbon (FC-01). Physical adsorption of the gas molecules to the walls of the pores was presented as a plausible cause of the behavior of gases in FC-01. Finally, the correlation was successfully applied to a set of experimental results obtained by other investigators.

6.2 Conclusion

In the study of the permeabilities of the FC-01 and FC-25 carbons with helium, nitrogen, argon and sulfur hexafluoride, it was found that:

1. Mean pressure alone does not uniquely define the permeability. Inlet pressure is also a variable.
2. Temperature gradient itself does not affect the permeability in these carbons. The decrease in the permeability when a temperature gradient is present is totally attributed to the mean temperature variations.
3. In the application of Carman and Arnell's model, the parameters B_0 and K_0 , given in Equations (2.4), were dependent on the gas properties. The nature of this dependence is not known.
4. The value of N in Somerville's model has some dependence on the particular gas used. Due to the complexity of this dependence, attempts at correlating N with the important gas parameters were not successful.
5. A new experimental correlation, given by Equation (5.2), adequately elucidates the effect of gas properties on the permeability.
6. The new correlation tends to indicate that physical adsorption may be a significant phenomenon which affects the permeability in the finer-pored sample.

6.3 Recommendations for Additional Work

The flow of gases with a wide range of physical properties through a given porous sample cannot only lead to a good understanding of the important gas parameters involved, but also point out the nature of the dependence of the permeability on the porous sample

itself. Additional experimental and theoretical work in this area would be of value.

A knowledge of the gas-porous medium system under transient flow conditions would also be of significant value in some engineering applications.

Finally, a study of the occurrence of physical adsorption and its effect on the permeability could elucidate some of the phenomena which occur in the flow of gases through fine-pored media.

BIBLIOGRAPHY

1. Orr, C., "Application of Mercury Penetration to Materials Analysis," Powder Technology, Vol. 3, (1969), p. 117.
2. Bickerman, J. J., Surface Chemistry, (New York: Academic Press, 1947, p. 322).
3. Somerville, M. H., "Non-Isothermal Gaseous Flow Through Fine-Pored Media," Ph.D. Thesis, Mechanical Engineering, The Pennsylvania State University, 1972.
4. Cha, C. Y., McCoy, B. J., "Application of Third-Order Constitutive Relations to Poiseuille Flow of a Rarefied Gas," The Journal of Chemical Physics, Vol. 54, (1971), p. 4373.
5. Adzumi, H., "On the Flow of Gases Through a Porous Wall," Bulletin of the Chemical Society of Japan, Vol. 12, 1937, p. 304.
6. Childs, E. C., Collis-George, N., "The Permeability of Porous Materials," Proceedings of the Royal Society, Vol. A201, 1950, p. 392.
7. Evans, R. B., Watson, G. M., Mason, E. A., "Gaseous Diffusion in Porous Media II, Effect of Pressure Gradients," Journal of Chemical Physics, Vol. 36, 1962, p. 1894.
8. Lammers, G. B., "The Application of Thermal Transpiration to a No-Moving Part Pump," Ph.D. Thesis, Mechanical Engineering, Case Western Reserve University, 1969.
9. Carman, P. C., and Arnell, J. C., "Surface Area Measurements of Fine Powders Using Modified Permeability Equations," Canadian Journal of Research, Vol. A-26, 1948, p. 128.
10. Kennard, E. H., Kinetic Theory of Gases, (New York: McGraw-Hill, 1937, p. 331).
11. Barrer, R. M., Strachan, E., "Sorption and Surface Diffusion in Microporous Carbon Cylinders," Proceedings of the Royal Society, Vol. A-231, 1955, p. 52.
12. Grove, D. M., "Permeability and Flow Studies," in Carbon, (New York: Academic Press, 1967, p. 155).
13. Hutcheon, J. M., Longstaff, B., Warner, R. K., in Society of Chemical Industry Symposium on Industrial Carbon and Graphite, 1958, p. 259.

APPENDIX

EXPERIMENTAL DATA

All the experiments were performed with an inlet pressure of 30 in. Hg absolute. All other flow parameters may be determined with the aid of the following tabular data.

Gas: Helium Porous Carbon: FC-01 $dT/dx = 0$ $T_m = 298^\circ K$		Gas: Helium Porous Carbon: FC-01 $dT/dx = 55^\circ K/cm$ $T_m = 412^\circ K$		Gas: Helium Porous Carbon: FC-01 $dT/dx = -58^\circ K/cm$ $T_m = 415^\circ K$	
$\dot{m} \times 10^4$ (gm/min)	Δp (in. Hg)	$\dot{m} \times 10^3$ (gm/min)	Δp (in. Hg)	$\dot{m} \times 10^4$ (gm/min)	Δp (in. Hg)
44.3	27.5	3.61	27.7	37.7	27.7
40.2	24.1	3.36	24.6	32.8	23.7
34.5	20.9	2.95	21.5	27.9	19.8
29.5	16.2	2.54	17.1	21.3	15.2
20.5	11.4	2.05	14.3	12.3	8.8
12.6	7.3	1.48	10.2	4.92	3.4
10.3	5.9	1.07	7.2	16.4	11.9
6.89	4.0			8.21	6.0
6.24	3.6				
25.4	13.6				

Gas: Helium Porous Carbon: FC-25 $dT/dx = 0$ $T_m = 298^\circ K$		Gas: Helium Porous Carbon: FC-25 $dT/dx = 38^\circ K/cm$ $T_m = 394^\circ K$		Gas: Helium Porous Carbon: FC-25 $dT/dx = -41^\circ K/cm$ $T_m = 395^\circ K$	
$\dot{m} \times 10^4$ (gm/min)	Δp (in. Hg)	$\dot{m} \times 10^4$ (gm/min)	Δp (in. Hg)	$\dot{m} \times 10^4$ (gm/min)	Δp (in. Hg)
128.	25.2	91.9	25.9	92.7	26.1
115.	22.2	83.7	22.6	82.9	23.3
108.	20.1	73.9	19.6	72.2	19.5
98.5	17.8	64.0	16.7	57.4	15.3
85.3	15.0	50.9	12.9	45.1	11.6
68.9	11.7	27.9	6.4	36.1	9.4
47.6	7.8	20.5	4.7	27.9	6.7
36.1	5.8	9.03	2.1	14.1	3.4
18.1	2.7	7.06	1.7	9.36	2.2
15.9	2.5	37.7	9.2	4.92	1.3
12.8	2.0	40.2	9.9		
5.74	1.0				

Gas: Nitrogen
Porous Carbon: FC-01
 $dT/dx = 0$
 $T_m = 298^\circ\text{K}$

$\dot{m} \times 10^3$ (gm/min)	Δp (in. Hg)
18.4	24.2
16.7	21.8
13.8	18.3
12.6	17.0
12.1	16.4
9.19	13.8
20.4	27.6
20.9	27.7
15.2	19.8
11.5	15.6
7.81	11.2
4.60	8.4

Gas: Nitrogen
Porous Carbon: FC-01
 $dT/dx = 84^\circ\text{K/cm}$
 $T_m = 433^\circ\text{K}$

$\dot{m} \times 10^3$ (gm/min)	Δp (in. Hg)
15.3	28.0
14.4	26.0
12.4	22.1
9.88	18.2
4.60	12.2
5.74	13.2
4.25	11.4
2.87	9.8
5.97	13.6
7.24	15.0

Gas: Nitrogen
Porous Carbon: FC-01
 $dT/dx = -79^\circ\text{K/cm}$
 $T_m = 428^\circ\text{K}$

$\dot{m} \times 10^2$ (gm/min)	Δp (in. Hg)
1.44	27.0
1.44	26.8
1.25	22.9
1.01	18.9

Gas: Nitrogen
Porous Carbon: FC-25
 $dT/dx = 0$
 $T_m = 298^\circ\text{K}$

$\dot{m} \times 10^2$ (gm/min)	Δp (in. Hg)
5.23	22.0
4.94	21.4
4.71	19.9
4.48	18.2
4.02	16.6
3.56	14.0
3.04	12.0
2.18	8.2
1.40	4.8
5.51	25.0
4.37	17.5
3.99	16.0

Gas: Nitrogen
Porous Carbon: FC-25
 $dT/dx = 34^\circ\text{K/cm}$
 $T_m = 391^\circ\text{K}$

$\dot{m} \times 10^2$ (gm/min)	Δp (in. Hg)
3.76	26.1
3.45	22.2
3.22	19.5
2.85	16.7
2.70	15.8
2.37	12.9
1.59	8.35
1.34	5.75
2.01	10.1

Gas: Nitrogen
Porous Carbon: FC-25
 $dT/dx = -51^\circ\text{K/cm}$
 $T_m = 403^\circ\text{K}$

$\dot{m} \times 10^2$ (gm/min)	Δp (in. Hg)
3.79	26.3
3.53	22.3
3.17	19.2
2.64	14.9
2.16	11.6
1.70	9.1
1.10	6.2

Gas: Argon
Porous Carbon: FC-01
 $dT/dx = 0$
 $T_m = 298^\circ\text{K}$

$\dot{m} \times 10^3$ (gm/min)	Δp (in. Hg)
16.4	28.1
15.4	26.0
13.6	23.2
11.5	19.2
10.0	16.7
7.39	11.8
4.60	7.7
5.09	8.4
12.5	21.0

Gas: Argon
Porous Carbon: FC-01
 $dT/dx = 82^\circ\text{K/cm}$
 $T_m = 421^\circ\text{K}$

$\dot{m} \times 10^3$ (gm/min)	Δp (in. Hg)
13.1	28.3
12.0	24.9
9.85	20.7
5.74	11.7
5.25	10.6
4.92	9.9
7.55	15.4

Gas: Argon
Porous Carbon: FC-01
 $dT/dx = -35^\circ\text{K/cm}$
 $T_m = 427^\circ\text{K}$

$\dot{m} \times 10^3$ (gm/min)	Δp (in. Hg)
13.1	28.3
11.8	25.2
10.2	22.1
6.07	12.8
4.92	10.4
9.06	19.9

Gas: Argon
Porous Carbon: FC-25
 $dT/dx = 0$
 $T_m = 298^\circ\text{K}$

$\dot{m} \times 10^3$ (gm/min)	Δp (in. Hg)
53.7	25.6
44.3	19.1
40.2	16.6
32.8	13.1
21.0	7.5
5.91	2.1
16.4	6.1
9.36	3.3
26.8	10.0
31.2	12.2
36.9	15.0
49.2	21.8

Gas: Argon
Porous Carbon: FC-25
 $dT/dx = 50$
 $T_m = 401^\circ\text{K}$

$\dot{m} \times 10^3$ (gm/min)	Δp (in. Hg)
36.9	26.3
35.3	24.3
30.4	18.9
25.4	14.2
15.6	8.6
7.39	3.8
22.2	12.2

Gas: Argon
Porous Carbon: FC-25
 $dT/dx = -41^\circ\text{K/cm}$
 $T_m = 397^\circ\text{K}$

$\dot{m} \times 10^3$ (gm/min)	Δp (in. Hg)
36.6	26.3
31.5	21.7
28.7	18.6
23.0	13.4
16.1	9.2
7.71	4.2

Gas: Sulfur Hexafluoride
 Porous Carbon: FC-01
 $dT/dx = 0$
 $T_m = 298^\circ\text{K}$

$\dot{m} \times 10^2$ (gm/min)	Δp (in. Hg)
4.19	28.1
3.89	26.2
3.71	24.6
3.44	22.8
2.70	15.4

Gas: Sulfur Hexafluoride
 Porous Carbon: FC-25
 $dT/dx = 0$
 $T_m = 298^\circ\text{K}$

$\dot{m} \times 10^2$ (gm/min)	Δp (in. Hg)
20.5	22.9
18.2	18.4
16.4	16.0
14.5	13.5
10.7	9.2
7.01	5.9
4.25	3.2
12.6	11.0
19.2	19.9
7.97	6.9